Ionic currents in intimal cultured synoviocytes from the rabbit

R. J. Large, M. A. Hollywood, G. P. Sergeant, K. D. Thornbury, S. Bourke, J. R. Levick and N. G. McHale

Am J Physiol Cell Physiol 299:C1180-C1194, 2010. First published 18 August 2010; doi:10.1152/ajpcell.00028.2010

You might find this additional info useful...

This article cites 67 articles, 34 of which can be accessed free at:
http://ajpcell.physiology.org/content/299/5/C1180.full.html#ref-list-1

This article has been cited by 1 other HighWire hosted articles

KCa1.1 Potassium Channels Regulate Key Proinflammatory and Invasive Properties of Fibroblast-like Synoviocytes in Rheumatoid Arthritis
Xueyou Hu, Teresina Laragione, Liang Sun, Shyny Koshy, Karlie R. Jones, Iskander I. Ismailov, Patricia Yotnda, Frank T. Horrigan, Pércio S. Gulko and Christine Beeton
J. Biol. Chem., February 3, 2012; 287 (6): 4014-4022.
[Abstract] [Full Text] [PDF]

Updated information and services including high resolution figures, can be found at:
http://ajpcell.physiology.org/content/299/5/C1180.full.html

Additional material and information about ***AJP - Cell Physiology*** can be found at:
http://www.the-aps.org/publications/ajpcell

This infomation is current as of March 8, 2012.

AJP - Cell Physiology is dedicated to innovative approaches to the study of cell and molecular physiology. It is published 12 times a year (monthly) by the American Physiological Society, 9650 Rockville Pike, Bethesda MD 20814-3991. Copyright © 2010 by the American Physiological Society. ISSN: 0363-6143, ESSN: 1522-1563. Visit our website at http://www.the-aps.org/.

Downloaded from ajpcell.physiology.org on March 8, 2012

Am J Physiol Cell Physiol 299: C1180–C1194, 2010.
First published August 18, 2010; doi:10.1152/ajpcell.00028.2010.

Ionic currents in intimal cultured synoviocytes from the rabbit

R. J. Large,[1] M. A. Hollywood,[1] G. P. Sergeant,[1] K. D. Thornbury,[1] S. Bourke,[1] J. R. Levick,[2] and N. G. McHale[1]

[1]*Smooth Muscle Research Centre, Dundalk Institute of Technology, Dundalk, Ireland; and* [2]*Physiology, Basic Medical Sciences, St George's Hospital Medical School, London, United Kingdom*

Submitted 28 January 2010; accepted in final form 12 August 2010

Large RJ, Hollywood MA, Sergeant GP, Thornbury KD, Bourke S, Levick JR, McHale NG. Ionic currents in intimal cultured synoviocytes from the rabbit. *Am J Physiol Cell Physiol* 299: C1180–C1194, 2010. First published August 18, 2010; doi:10.1152/ajpcell.00028.2010.—Hyaluronan, a joint lubricant and regulator of synovial fluid content, is secreted by fibroblast-like synoviocytes lining the joint cavity, and secretion is greatly stimulated by Ca^{2+}-dependent protein kinase C. This study aimed to define synoviocyte membrane currents and channels that may influence synoviocyte Ca^{2+} dynamics. Resting membrane potential ranged from −30 mV to −66 mV (mean −45 ± 8.60 mV, $n = 40$). Input resistance ranged from 0.54 GΩ to 2.6 GΩ (mean 1.28 ± 0.57 GΩ; $\nu = 33$). Cell capacitance averaged 97.97 ± 5.93 pF. Voltage clamp using Cs^+ pipette solution yielded a transient inward current that disappeared in Ca^{2+}-free solutions and was blocked by 1 μM nifedipine, indicating an L-type calcium current. The current was increased fourfold by the calcium channel activator FPL 64176 (300 nM). Using K^+ pipette solution, depolarizing steps positive to −40 mV evoked an outward current that showed kinetics and voltage dependence of activation and inactivation typical of the delayed rectifier potassium current. This was blocked by the nonspecific delayed rectifier blocker 4-aminopyridine. The synoviocytes expressed mRNA for four Kv1 subtypes (Kv1.1, Kv1.4, Kv1.5, and Kv1.6). Correolide (1 μM), margatoxin (100 nM), and α-dendrotoxin block these Kv1 subtypes, and all of these drugs significantly reduced synoviocyte outward current. The current was blocked most effectively by 50 nM κ-dendrotoxin, which is specific for channels containing a Kv1.1 subunit, indicating that Kv1.1 is critical, either as a homomultimeric channel or as a component of a heteromultimeric Kv1 channel. When 50 nM κ-dendrotoxin was added to current-clamped synoviocytes, the cells depolarized by >20 mV and this was accompanied by an increase in intracellular calcium concentration. Similarly, depolarization of the cells with high external potassium solution caused an increase in intracellular calcium, and this effect was greatly reduced by 1 μM nifedipine. In conclusion, fibroblast-like synoviocytes cultured from the inner synovium of the rabbit exhibit voltage-dependent inward and outward currents, including Ca^{2+} currents. They thus express ion channels regulating membrane Ca^{2+} permeability and electrochemical gradient. Since Ca^{2+}-dependent kinases are major regulators of synovial hyaluronan secretion, the synoviocyte ion channels are likely to be important in the regulation of hyaluronan secretion.

L-type calcium; synovium

SYNOVIAL FLUID AND THE SYNOVIAL lining (synovium) are crucial for normal diarthrodial joint function, both for cartilage nutrition and for tissue lubrication. Synovium is a richly vascularized, very thin sheet of cells comprising both fibroblast-like synoviocytes (FLS) and macrophages. The FLS strongly expresses hyaluronan (HA) synthase 2 (HAS2) and secretes the glycosaminoglycan HA (molecular weight 2,000–6,000) into the joint cavity and synovial intercellular spaces. HA acts as a viscous lubricant under low load, hydrodynamic conditions. HA also helps retain synovial fluid in the joint cavity via an osmotic, concentration polarization mechanism (47, 61, 63) and by greatly reducing the permeability of the intercellular fluid exchange pathway (62). The concentration of intra-articular HA is greatly reduced in osteo- and rheumatoid arthritis. Studies of HA secretion into rabbit joints in vivo showed that secretion can be stimulated by joint distension, cyclic movement, and protein kinase C activation, as well as by other factors (1, 14, 29, 30, 68). Studies of cultured synoviocytes from the innermost synovial lining (intima) have implicated Ca^{2+} entry and classic Ca^{2+}-dependent protein kinase C-α (Ca-PKCα) in HA regulation (52, 53), and confirmed that synoviocyte HA secretion is a mechanosensitive process.

The above findings focus attention on the regulation of synoviocyte Ca^{2+} content and highlight the need for a better understanding of the basic cellular physiology and electrophysiology of synoviocytes. The key role of FLS cells in the pathogenesis of rheumatoid arthritis reinforces this need (28). In HIG-82 cells, which are an immortalized cell line derived from peri-articular tissue and are, unlike true synoviocytes, rich in gap junctions, interleukin-1β partly depolarizes the cells via a PKC- and nifedipine-sensitive process (39, 40). Synovial sarcoma cell line SW982 expresses transient receptor potential (TRP) type V (TRPV) and L-type Ca^{2+} channels (37) and store-mediated Ca^{2+} transients (12). Also, some fibroblasts (from which synoviocytes appear to be derived) have mechanically modulated membrane potentials, stretch-activated nonselective cation channels, stretch-activated Ca^{2+} influx, verapamil-sensitive Ca^{2+}, voltage-gated K^+ and large-conductance calcium-activated K^+ channels (17, 20, 34, 35, 38, 71). Cardiac fibroblasts appear to lack L-type Ca^{2+} channels but express TRPC nonselective cation-conducting channels (60), delayed rectifier channels (67), and stretch-activated channels (9). While it would be unwise to assume that the rabbit intimal FLS have identical properties to fibroblasts, there is circumstantial evidence of similarities. For example, Momberger et al. (53) showed that rabbit intimal FLS secretion of HA is both stretch sensitive and calcium dependent in vitro; also Bay K 8644 (Bay K), which opens L-type calcium channels, stimulates FLS secretion of HA in vitro. Moreover, injection of the calcium ionophore ionomycin into the rabbit synovial joint increases HA secretion in vivo (30). To date, however, there have been no direct electrophysiological studies to demonstrate and characterize calcium channels in selectively prepared, intimal FLS cells. The same is true for potassium channels, which are likely to be important in the control of membrane potential in cells and hence the electrochemical gradient for extracellular Ca^{2+} entry. The time is ripe, therefore, to determine what currents are expressed in intimal FLS cells and for a detailed electrophysiological study to characterize them.

Address for reprint requests and other correspondence: N. G. McHale, Smooth Muscle Research Centre, Dundalk Institute of Technology, Dublin Road, Dundalk, Co Louth, Ireland (e-mail: noel.mchale@dkit.ie).

0363-6143/10 Copyright © 2010 the American Physiological Society

Downloaded from ajpcell.physiology.org on March 8, 2012

MATERIALS AND METHODS

Selective Tissue Harvest and Cell Culture

All experiments were approved by the Dundalk Institute of Technology Animal Use and Care Committee. The synovium was microdissected from healthy New Zealand White rabbits immediately after they had been killed by lethal intravenous pentobarbitone sodium. The joint cavity was cut open and flushed gently with Ca^{2+}-free Hanks' solution to maintain hydration during dissection. The synovial lining (intima) from the lateral and medial sides of the suprapatellar zone was microdissected from the underlying areolar subsynovium with ultrafine ophthalmic precision instruments (John Weiss, London, UK). The method adopted was that of Price et al. (56), in which only the innermost, ~20 μm thick layer (the true, FLS-rich synovial layer or intima) is harvested; gross dissection, by contrast, harvests also the less specialized, much thicker (>100 μm) subsynovial connective tissue. The selectively harvested intima was chopped into even smaller pieces for primary explant culture. The explants were transferred to a T-25 tissue culture flask (Corning) and cultured for 24 h in 1 ml Ham's F-12 medium (Khaign's modification, Gibco) supplemented with 30% fetal calf serum (FCS, Gibco) and 2% penicillin/streptomycin/fungizone (PSF, Gibco). Medium supplemented with 20% FCS and 2% PSF was added over the next 5 days at 1 ml per day. An initial cellular outgrowth was observed after 4 days culture, with medium being changed every 2 days after *day 6*. This was maintained until confluence when the tissue fragments were removed. The synovial lining cells were cultured and reseeded. Cells were used for experiments upon reaching *passage 6* (P6).

Characterization of Synovial Lining Cells In Situ and After Culture

Nonspecific esterase staining for macrophages. Macrophages account for approximately one third of the surface-lining cells in rabbit synovium and strongly express nonspecific esterase (NSE) (16), whereas the FLS cells, ~67% of the surface-lining cells (45), show little to no NSE activity. Macrophages disappear from culture with repeated passage. To confirm this, NSE assay was performed using a commercially available kit (Sigma). Cultured synoviocytes from P2 and P7 were plated onto glass-bottomed petri dishes and allowed to adhere for 24 h. Cells were fixed by submersion in a citrate-acetone-formaldehyde solution at room temperature for 30 s, then washed with deionized water before application of a reaction solution containing α-napthyl acetate for 30 min at 37°C. Cells were again washed with deionized water, followed by application of hematoxylin solution Gill no. 3 for 2 min. Finally, the cells were washed with deionized water and viewed under a Zeiss LSM 510-Meta confocal microscope. The presence of NSE results in a dark-blue/black granulation of cells.

Immunohistochemical studies for vimentin and Kv1.1 expression. To further characterize the cells under study, whole mount, microdissected preparations of synovium were pinned flat on Sylgard mounting dishes and single cell preparations were cultured on 35-mm glass-bottomed culture dishes. Culture medium was removed before staining, and cells were washed three times for 5 min in phosphate-buffered saline (PBS). Tissue and cells were fixed with PBS containing 4% paraformaldehyde for 1 h and 10 min, respectively, and washed three times in PBS for 5 min before immunohistochemical labeling. To minimize nonspecific binding of goat secondary antibody, tissue/cells were preincubated for 1 h in PBS containing 5% normal goat serum (Sigma-Aldrich) and for 10 min in 1% Triton X-100 to enhance penetration of antisera. Specimens were washed three times in PBS for 5 min and incubated in PBS containing mouse monoclonal anti-vimentin (1:8,000, Sigma-Aldrich, V6630) or mouse monoclonal anti-Kv1.1 (Neuromabs, University of California, Davis) and 0.1% normal goat serum overnight at 4°C. Following incubation, excess antibody was removed by washing in PBS times for 5 min. Samples were incubated with PBS containing anti-mouse Alexa Fluor 488 secondary antibody (1:1,000, Invitrogen Molecular Probes) and 0.1% normal horse serum for 1 h at room temperature. Samples were washed in PBS three times for 5 min before imaging, to remove any unbound secondary antibody. Images were captured on an upright Zeiss Meta 510 laser confocal system with water dipping immersion objective lens. The specimens were excited with an argon laser to excite fluorophores at 488 nm, and emission filters enabled collection at 520 nm (green). Images were acquired and reconstructed using the Zeiss LSM software.

Total RNA isolation and RT-PCR for HAS2 and Kv1 expression. RNA isolated from cultured synoviocyte cells (P6) and freshly dissected synovium was assessed for HAS2 mRNA, since HAS2 is highly expressed in intimal FLS cells (52, 54). Total RNA was prepared from synovium using the TRIzol method (Invitrogen) as per manufacturer's instructions and treated with DNase (Stratagene). Total RNA was obtained from synoviocyte cell cultures using an RNeasy Micro Kit (Qiagen). Briefly, cells were grown to confluence in T25-cm^2 culture flasks and subsequently washed and collected in cell lysis buffer. Lysed cells were treated as per manufacturer's instructions. First-strand cDNA was prepared from the RNA preparations using the Superscript II RNase H reverse transcriptase (Invitrogen); 200 μg/ml of random hexamer was used to reverse transcribe the RNA sample. The cDNA reverse transcription product was amplified with specific primers by PCR. PCR was performed in a 25-μl reaction containing 12.5 μl Amplitaq Gold Mastermix (Applied Biosystems), 8.5 μl of water, 1 μl of sense and antisense primers at 10 μM, and 2 μl of template cDNA. All reactions were performed in a Techne TC-512 gradient thermal cycler. The amplification profile for all primer pairs was as follows: 95°C for 5 min, followed by 35 cycles of 95°C for 30 s and 58°C for 1 min, with a final extension step at 72°C for 7 min. The amplified products were separated by electrophoresis on a 2% agarose-1 × TAE (Tris, acetic acid, EDTA) gel, and the DNA bands were subsequently visualized by ethidium bromide staining and documented on an INGENIUS gel documentation system (Syngene Bio Imaging). Details of primers used in this study are contained in Table 1.

Table 1. *Primers used for RT-PCR*

Amplicon	Forward	Reverse	Source
HAS2 409	TTT CTT TAT GTG ACT CAT CTG TCT CAC CGG	ATT GTT GGC TAC CAG TTT ATC CAA ACG G	Ref. 53
Kv1.1 235	ATT GTG GCC ATC ATC CCT TA	CGC CAA TGA AGA GGA AAA AG	Designed
Kv1.2 400	GCA GCT GGA AGG CGT A	TCT CCA TGG CCT CCT CA	Designed
Kv1.3 397	AAC GTG CCC ATC GAC A	GAG CAG CTC GAA GGA GA	Designed
Kv1.4 288	CTT CCT CTT CAT TGG GGT CA	AGC TGC GTC TGT TCC TCA TT	Designed
Kv1.5 181	ACG AGT ACT TCT TCG ACC GCA ACC G	TTG ATG AAG CCC TCG TCC TCC C	Designed
Kv1.6 96	GAC CTG AAG GCA ACG GAC AAT	CGA TGT GGA GTT GGA AGG TAG C	Ref. 55a
Kv1.7 250	TGC CCT TCA ATG ACC CGT TCT TC	AAG ACA CGC ACC AAT CGG ATG AC	Designed
Kv1.8 250	ATC TCC ATC GTC ATC TTT TG	GGG ATG ATG GAG ATG ATG TC	Designed

HAS2, hyaluronan synthase 2.

Downloaded from ajpcell.physiology.org on March 8, 2012

Calcium Imaging

Cells were cultured overnight in glass-bottomed petri dishes. They were then incubated in 0.4 μM fluo-4 AM (Molecular Probes) in Hanks' solution containing 100 μM Ca^{2+} and 1 mM probenecid for 10–12 min in the dark at room temperature. Cells were imaged using an iXon 887 EMCCD camera (512 pixels × 512 pixels; Andor Technology, Belfast, Ireland) coupled to a Nipkow spinning disk confocal head (CSU22, Yokogawa, Japan). A krypton-argon laser (Melles Griot UK) at 488 nm was used to excite the fluo-4, and the emitted light was detected at wavelengths >510 nm. Experiments were performed using a ×40 objective (Olympus), and images were acquired at five frames per second. Background fluorescence from the camera, obtained using a null frame, was subtracted from each frame to obtain 'F'. F_0 was determined as the minimum fluorescence measured between oscillations under control conditions. To obtain post hoc linescan images for display of the calcium response, a 1 pixel-thick line was drawn centrally through the entire length of the cell and the "reslice" command in ImageJ (National Institutes of Health, Bethesda, MD) was invoked. Plots of F/F_0 were obtained from the post hoc linescan by drawing a rectangle around the entire area of the linescan image and plotting the intensity profile in ImageJ.

Electrophysiology

For electrophysiological experiments the cells were trypsinized and reseeded on the day of experimentation. Cells were detached from the surface of the culture flask by two initial washes with Ca^{2+}/Mg^{2+}-free PBS (Gibco) followed by a 3-min exposure to 0.75 ml trypsin-EDTA (Gibco) at 37°C. Displaced cells were collected in 8 ml of fresh Ham's F-12 medium and either reseeded in a T-25 culture flask, or plated in 35-mm^3 dishes for electrophysiological studies. During these experiments the dish containing the cells was continuously perfused with Hanks' solution at 36 ± 1°C. Additionally, the cell under study was continuously superfused by means of a custom built close delivery system with a pipette of tip diameter 200 μm placed ~300 μm from the cell. The Hanks' solution in the close delivery system could be switched to a drug-containing solution with a dead-space time of <5 s.

Perforated patch recordings from single cells. Currents were recorded using the perforated patch configuration of the whole cell patch-clamp technique (58). This circumvented the problem of current rundown encountered using the conventional whole cell configuration. The cell membrane was perforated using the antibiotic amphotericin B (600 μg/ml). Patch pipettes were initially front-filled by dipping into pipette solution and then back filled with the amphotericin B-containing solution. Voltage-clamp commands were delivered via an Axopatch 1D patch clamp amplifier (Axon Instruments), and membrane currents were recorded by a 12-bit AD/DA converter (Axodata 1200 or Labmaster - Scientific Solutions) interfaced to an AT-type computer running pClamp software.

Solutions. Solution composition was as follows (in mM). *1*) Hanks' solution contained 125 NaCl, 5.36 KCl, 10 glucose, 2.9 sucrose, 4.17 $NaHCO_3$, 0.44 KH_2PO_4, 0.33 Na_2HPO_4, 0.5 $MgCl_2$, 1.8 $CaCl_2$, 0.4 $MgSO_4$, and 10 HEPES; pH was adjusted to 7.4 with NaOH. *2*) Calcium-free Hanks' solution contained 125 NaCl, 5.36 KCl, 10 glucose, 2.9 sucrose, 4.17 $NaHCO_3$, 0.44 KH_2PO_4, 0.33 Na_2HPO_4, 2.3 $MgCl_2$, 5.0 EGTA, 0.4 $MgSO_4$, and 10 HEPES; pH was adjusted to 7.4 with NaOH. *3*) Cesium pipette solution contained 132.96 CsCl, 1.0 $MgCl_2$, 0.5 EGTA, and 10 HEPES; pH was adjusted to 7.2 with CsOH. *4*) Potassium pipette solution contained 132.96 KCl, 1.0 $MgCl_2$, 0.5 EGTA, and 10 HEPES; pH was adjusted to 7.2 with KOH.

Drugs. The following drugs were used: amphotericin B (Sigma), nifedipine (Tocris), FPL-64176 {methyl 2,5-dimethyl-4-[2-(phenylmethyl)benzoyl]-1H-pyrrole-3-carboxylate; Tocris; FPL}, 4-aminopyridine (4-AP, Sigma), tetraethylammonium chloride (TEA, Sigma), correolide (Merck), margatoxin (Alamone Labs), α-dendroxin (Sigma), and κ-dendrotoxin (Sigma). All drugs were made up in the appropriate stock solution before being diluted to their final concentrations in Hanks' solution.

Statistical analysis. In all experiments, *n* refers to the number of cells studied. Summary data are presented as means ± SD (in the case of the passive electrical properties) or means ± SE (in all other cases), and statistical comparisons were made on raw data using Student's paired *t*-test, taking $P < 0.05$ level as significant.

RESULTS

Cell Characterization

The synovial intima contains a substantial proportion of monocyte-derived macrophages (~33%) in addition to the fibroblast-like synoviocytes (~67%), plus a smaller proportion of vascular cells (45), so it was important at the outset to define the cells being studied. The FLS cells are NSE negative; are vimentin positive; bind MAb 67 (7, 64) and synthesize and secrete hyaluronan via HAS2. The macrophages can be distinguished by their strong NSE positivity (16). A whole mount of a microdissected synovial sheet was stained with an antibody against vimentin and imaged using the confocal microscope (Fig. 1*A*). The vimentin-positive cells varied in morphology from ovoid through fibroblastoid to stellate. The cytoplasm and cytoplasmic projections were filled with vimentin filaments. These cells were very similar in shape and distribution to those described by McDonald and Levick (49) as type B synoviocytes.

When cells were cultured from the microdissected synovial membrane, the first passage yielded a mixed culture of macrophages and FLS (Fig. 1, *B* and *C*). The small, rounded cells (diameter <50 μm) were vimentin negative, whereas the elongated, stellate cells (typically 100–200 μm in length) were vimentin positive (Fig. 1*C*). The small round cells stained intensely for NSE, whereas the larger, stellate cells were NSE negative (Fig. 1*D*, *top*). By *passage 7* all of the NSE-positive cells had disappeared, leaving only the larger cells (Fig. 1*D*, *bottom*). To confirm that the remaining cells were FLS, cells from *passage 6* (similar to the cells used for electrophysiological and imaging studies) were subjected to total RNA extraction using the RNeasy Micro Kit. Total RNA was also prepared from freshly dissected synovium using the TRIzol method. The transcription product was amplified with primers specific for HAS2, and the resulting cDNA bands are shown in Fig. 2. HAS2 message was evident in both the *passage 6*-cultured synoviocytes and in intact synovium at dilutions of 1:1 and 1:5 but was absent from the nontemplate control (NTC). The panels at the bottom of the figure show the fixed erythrocyte exclusion test. Under normal conditions the synoviocytes were surrounded by a clear area from which erythrocytes were excluded (Fig. 2*B*, *bottom left*). This clear area disappeared after hyaluronidase addition, suggesting that it was due to hyaluronan secretion by the synoviocyte. The black calibration bar represents 20 μm in each case. Taken together, the above results gave us confidence that the cells studied were true fibroblast-like synoviocytes.

Synoviocyte Membrane Potential and Passive Electrical Properties

Resting membrane potential, measured in zero current-clamp mode using K^+-filled electrodes immediately after establishment of a gigaohm seal, ranged from −30 mV to −66

Downloaded from ajpcell.physiology.org on March 8, 2012

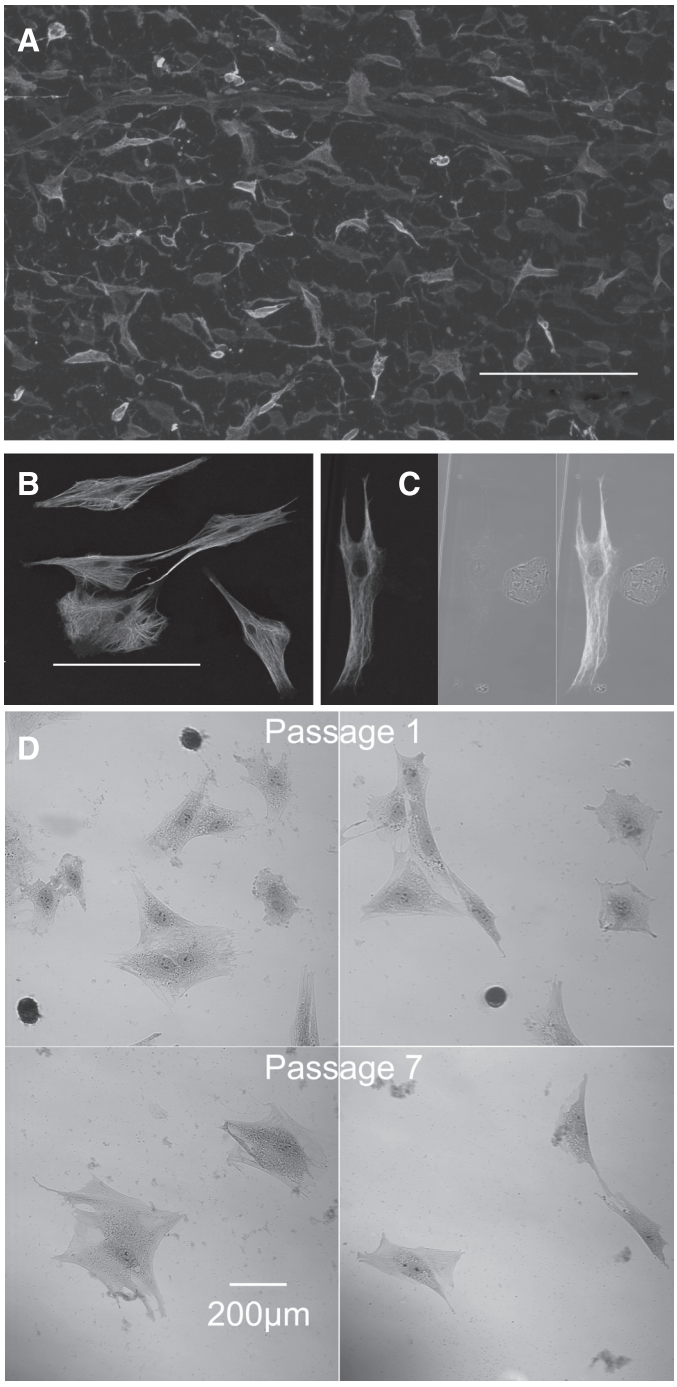

Fig. 1. *A*: whole mount of synovial intima stained with antibody against vimentin. The apparent differences in intensity of staining are due to the relative position in the confocal stack of the vimentin-stained cells. These varied in morphology from ovoid through fibroblastoid to stellate. The horizontal bars in each case indicate 200 μm. *B* and *C*: cultured cells from the first passage also stained with antibody against vimentin. *B*: confocal image of stellate cells rich in vimentin filaments, taken to be type B synoviocytes. *C*: vimentin-stained cell under laser illumination (*left*), a smaller rounded cell under bright field illumination (*middle*), and an overlay of both (*right*). No evidence of vimentin staining was seen in the small rounded cells, which we took to be macrophages. This conclusion was reinforced by nonspecific esterase (NSE) staining. *D*: the small rounded cells were strongly NSE positive while the larger cells were negative (*top*). When the staining was repeated in cells taken from *passage 7*, no NSE-positive cells were found (*bottom*).

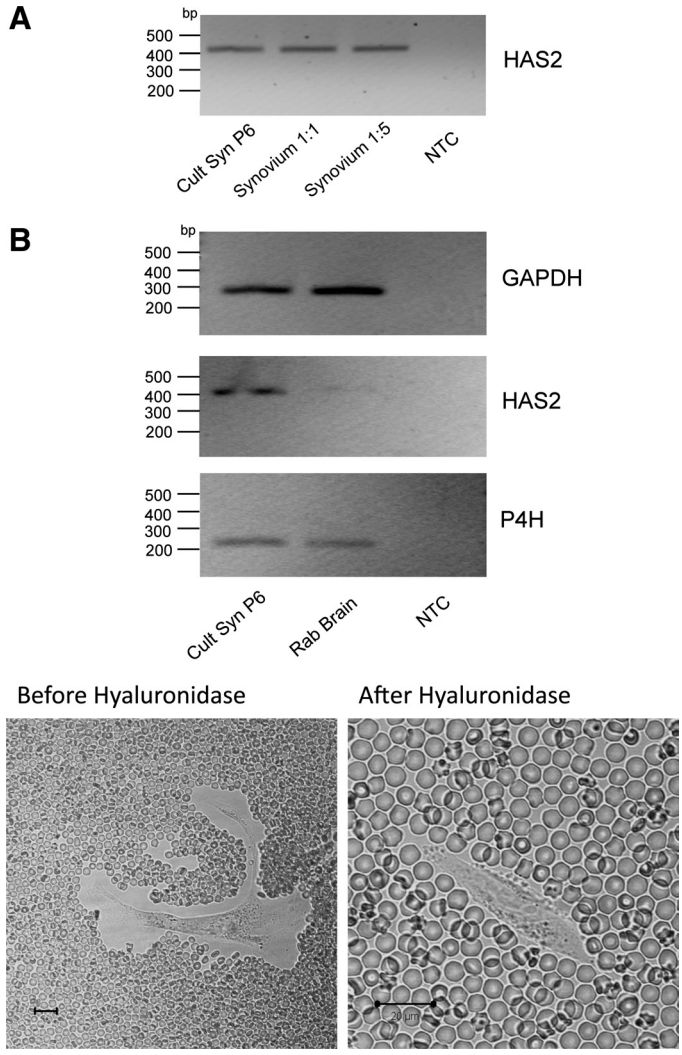

Fig. 2. Cells from *passage 6* (the passage used for electrophysiological studies) were subjected to total RNA extraction using the RNeasy Micro Kit. Total RNA was also prepared from freshly microdissected synovium using the TRIzol method. *A*: the transcription product was amplified with primers specific for hyaluronan synthase 2 (HAS2), and the resulting DNA bands are shown. HAS2 message was evident in both the *passage 6*-cultured synoviocytes (Cult Syn P6) and in intact synovium at dilutions of 1:1 and 1:5 but absent from the nontemplate control (NTC). *B, bottom*: fixed erythrocyte exclusion test. Under normal conditions the synoviocytes were surrounded by a clear area from which erythrocytes were excluded. This clear area disappeared after hyaluronidase addition, suggesting that it was due to hyaluronan secretion by the synoviocyte. Rab, rabbit; P4H, prolyl 4-hydroxylase. Black calibration bar represents 20 μm in each case.

mV with a mean of −45 ± 8.6 (SD, n = 40; Fig. 3) These values are relatively large when compared with cardiac fibroblasts, −25 to −35 mV (34) but lower than excitable cells such as cardiac myocytes. Input resistance was measured in 33 cells in voltage-clamp mode by measuring the passive current responses to a series of hyperpolarizing and depolarizing voltage steps from a holding potential of −60 mV. The input resistance ranged from 0.54 to 2.6 GΩ with a mean of 1.28 ± 0.57 (SD; Fig. 3). Cell capacitance was calculated by integrating the capacitative current evoked by small hyperpolarizing and depolarizing steps and dividing by the amplitude of the voltage change. The capacitance averaged 97.97 ± 5.93 pF (SD, n =

Downloaded from ajpcell.physiology.org on March 8, 2012

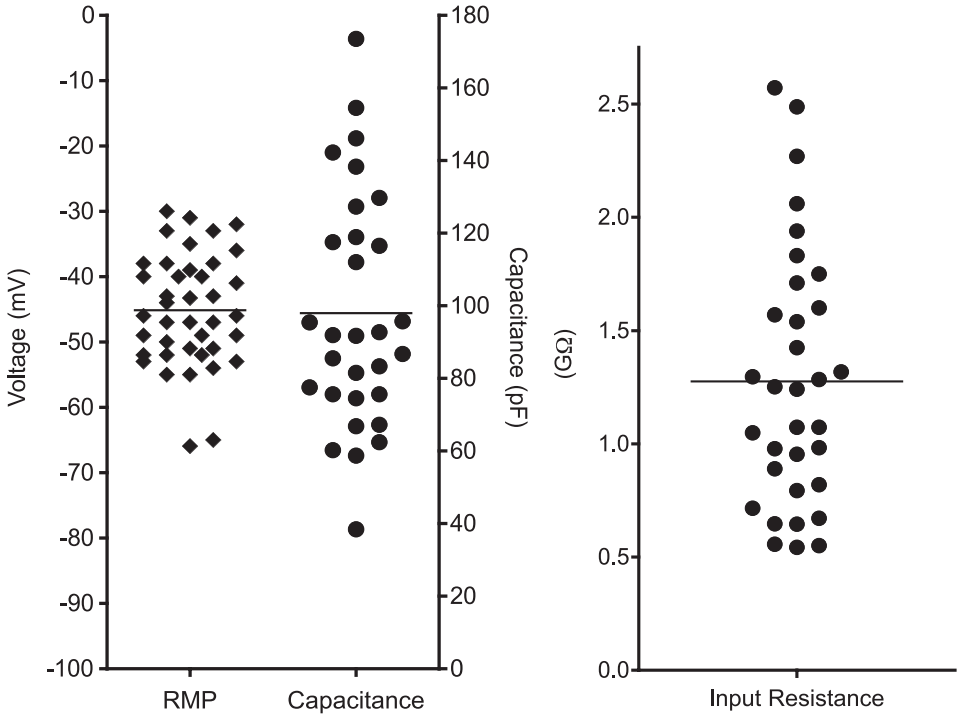

Fig. 3. The range of membrane potential measured in zero current clamp mode is shown for 40 cells. Values ranged from −30 mV to −66 mV with a mean of −45 mV. There was no clear bimodal distribution, indicating a fairly homogenous cell population. The measured capacitance ranged from <40 to ~180 pF, with a mean of 97.97 pF, reflecting the large variations in surface area of cultured cells. The mean input resistance was 1.27 GΩ with a range of 0.54 to 2.6 GΩ. RMP, resting membrane potential.

30; Fig. 3). These values are of a similar order of magnitude to those seen in cultured human cardiac fibroblasts, 49 ± 12.1 pF (46), but much larger than the values measured in acutely dissociated cells, 18 ± 3 pF (35), indicating that the cultured cells have a greater surface area perhaps due to their development of numerous cellular processes or membrane invaginations.

Inward Currents; Evidence for L-Type Ca^{2+} Channels in Synoviocytes

Voltage-clamp experiments were performed using Cs^+-filled pipettes (Cs^+ blocks currents carried by potassium ions) to characterize the inward currents evoked by depolarization. Cells were held at −80 mV and subjected to a series of 500-ms test pulses ranging from −80 to +50 mV. Figure 4*A* shows the family of currents evoked by this protocol. At voltages positive to −20 mV, a transient inward current was evoked that peaked within 5 ms and relaxed to 0 within 200 ms. This current was partially offset by an outward current that activated over the same voltage range and was likely to be due to cesium ions being carried through potassium channels. When these experiments were repeated using calcium-free solution, the transient inward current was abolished, leaving only the offsetting outward current (Fig. 4*B*). Confirmation that the latter current was carried through potassium channels was provided in a separate set of experiments where 1 mM tetraethylammonium (TEA) reduced the offsetting current (at the end of the +40-V step) by 67% ± 4% (mean ± SE, $n = 4$). Six experiments like those shown in Fig. 4, *A* and *B*, are summarized in Fig. 4*C*. The current-voltage (*I-V*) relationship was typical of L-type currents in other tissues in that peak current increased at voltages positive to −20 mV, reached a maximum at 0 mV, and reversed just under +30 mV (closed squares), which is less positive than one might expect and is undoubtedly due to contamination by outward Cs^+ current. In calcium-free solution, inward current was abolished, leaving only the offsetting outward current described above (closed triangles). This indicated that the inward current was carried by calcium ions.

Voltage-dependent inactivation of the inward current was investigated by holding cells at a series of conditioning potentials from −100 mV to +10 mV for 2 s before stepping to a test potential of 0 mV for 500 ms. Inactivation curves were constructed from these double pulse protocols by normalizing the current (I) during each test step to the maximum current (I_{max}) and then plotting (I/I_{max}) against the conditioning potential. The data were fitted with a Boltzmann equation of the form:

$$I/I_{max} = A + (B - A)/\{1 + \exp[(V_{1/2} - V_m)/K]\}$$

where K is the slope factor, $V_{1/2}$ is the voltage at which there is half-maximal inactivation, V_m is the conditioning potential, and A and B are constants corresponding to the top and bottom of the curve. This yielded a $V_{1/2}$ of inactivation of −26 ± 1.68 mV.

Activation curves were constructed from the *I-V* relationships by first calculating conductance, G, from: $G = I/(V_m - E_{rev})$, where V_m is the test potential and E_{rev} is the reversal potential for the current. The conductance was then normalized to the maximum value (G_{max}) and plotted as G/G_{max} against the test potential.

The experiments shown in Fig. 5, *A–C*, show the effect of the L-type Ca^{2+} channel blocker nifedipine (1 μM). The transient inward current was blocked by nifedipine, indicating that it was an L-type calcium current, in accord with the calcium-free experiments of Fig. 4. Figure 5*C* summarizes six such experiments. Mean inward current peaked at 0 mV and reversed at +23 mV. In the presence of nifedipine, inward

Downloaded from ajpcell.physiology.org on March 8, 2012

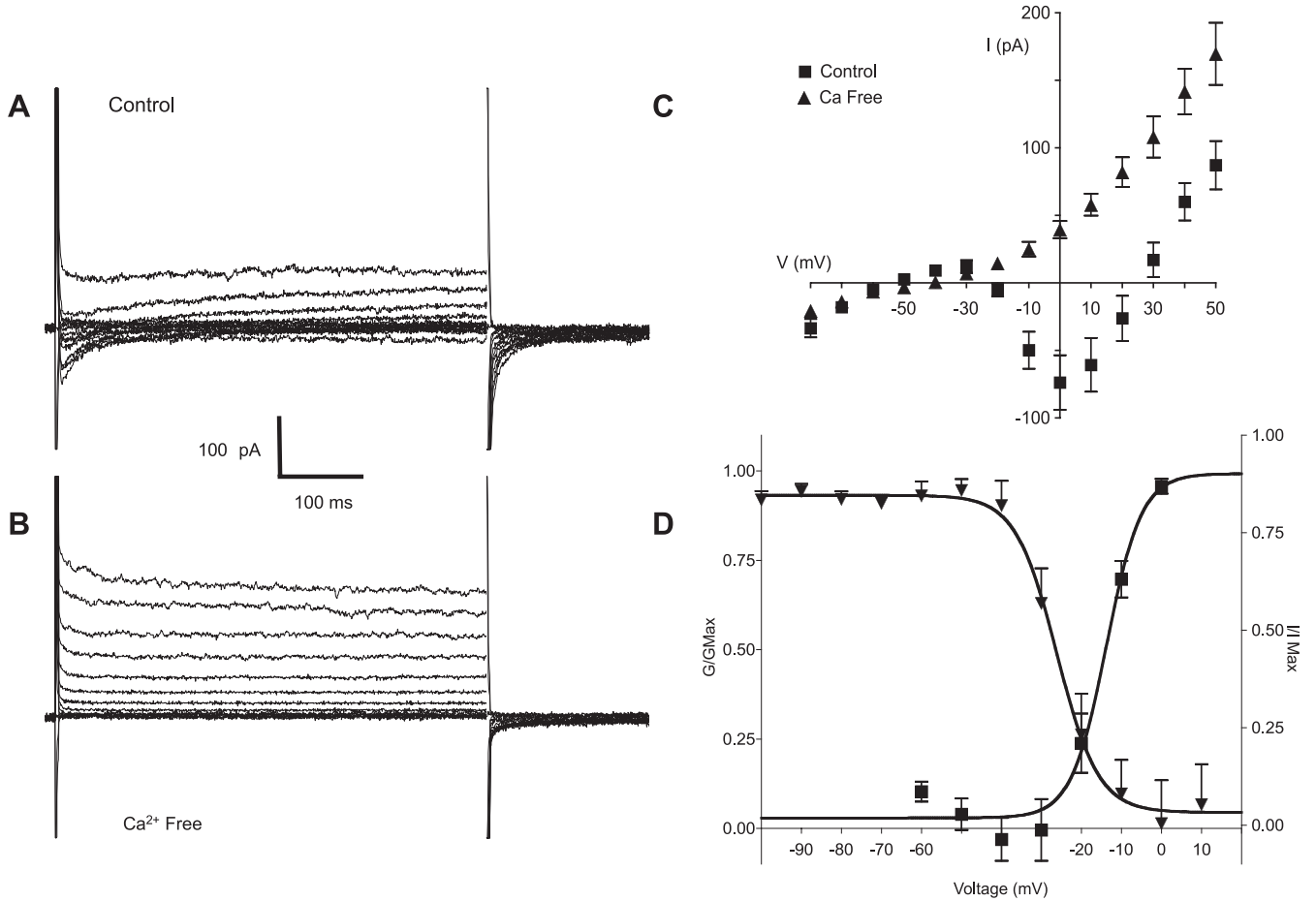

Fig. 4. *A*: family of currents elicited by holding the cell at −80 mV and stepping through a series of voltages from −80 mV to +50 mV in normal Hanks' solution. K^+ ions in the pipette solution were replaced with Cs^+ to block K^+ currents. At voltages positive to −20 mV, a transient inward current was evoked that peaked within 5 ms and relaxed to 0 within 200 ms. This current was partially offset by an outward current that activated over the same voltage range and was likely to be due to cesium ions being carried through potassium channels. *B*: same protocol as in *A* applied to the same cell but this time in Ca^{2+} -free Hanks' solution. The transient inward current was abolished, leaving only the outward current carried by Cs^+. *C*: current-voltage (*I-V*) relationship of the inward current is summarized in the plot of the mean results of six such experiments. Peak inward current (■) developed at voltages positive to −20 mV, reached a maximum at 0 mV, and reversed at just under +30 mV. In Ca^{2+}-free Hanks' solution (▲) the inward current was abolished at all voltages. *D*: voltage dependence of activation (■) and inactivation (▲) of the inward current. The mean results of 14 experiments were fitted with a Boltzmann equation giving a half-maximal voltage ($V_{1/2}$) of activation of −14 ± 1.7 mV. The current activated at voltages positive to −10 mV and was maximally active at voltages positive to 0 mV. Voltage-dependent inactivation was investigated by holding cells at a series of conditioning potentials from −100 mV to +10 mV for 2 s before stepping to a test potential of 0 mV for 500 ms. For analysis, the peak current at 0 mV was measured at each conditioning potential, normalized to the maximum current (I_{max}), and plotted against the appropriate potential. Mean data points in 5 such experiments were again fitted with a Boltzmann equation, yielding a $V_{1/2}$ of inactivation of −26 ± 1.68 mV. It is clear from this plot that availability of the inward current was high over the measured range of resting membrane potential. G_{max}, maximum conductance.

current was abolished, leaving only the outward current carried by Cs^+.

FPL is a calcium channel modulator specific for the L-type family of voltage-gated calcium channels (6, 66). Like the more commonly used agonist Bay K, FPL prolongs the opening of single calcium channels during depolarization and slows channel closing upon repolarization. We therefore examined its effects on the currents described above. The control inward currents (Fig. 5*D*) were greatly enhanced by 300 nM FPL (Fig. 5*E*). This was accompanied by somewhat slower activation kinetics and by very much slower inactivation (τ of inactivation, at 0 mV, increased from a mean of 36.8 ± 8.5 to 269 ± 41 in FPL), such that the currents were not fully inactivated at the end of the 500-ms sweep (Fig. 5*E*). A summary of 12 such experiments (Fig. 5*F*) shows that the mean peak inward current increased in amplitude and that the voltage at which current peaked shifted negatively by 10 mV. Peak inward current increased by 308% from 93 ± 17 pA to 380 ± 58 pA ($n = 12$; $P < 0.001$). The large FPL-induced inward current was reduced from −258 ± 81 to −9.2 ± −9.4 pA ($n = 6$; $P < 0.001$) following application of 1 μM nifedipine or upon switching to a calcium-free extracellular solution (−305 ± 84 to 25 ± 8 pA, $n = 6$; $P < 0.001$).

Outward Currents; Characterization of Potassium Channels in Synoviocytes

When the pipette solution was changed to one containing 132.96 mM K^+ and the protocol described above was applied, a family of outward currents was observed. These activated rapidly and then relaxed slowly throughout the remainder of the 500-ms test pulse (Fig. 6*A*). The currents were greatly

Downloaded from ajpcell.physiology.org on March 8, 2012

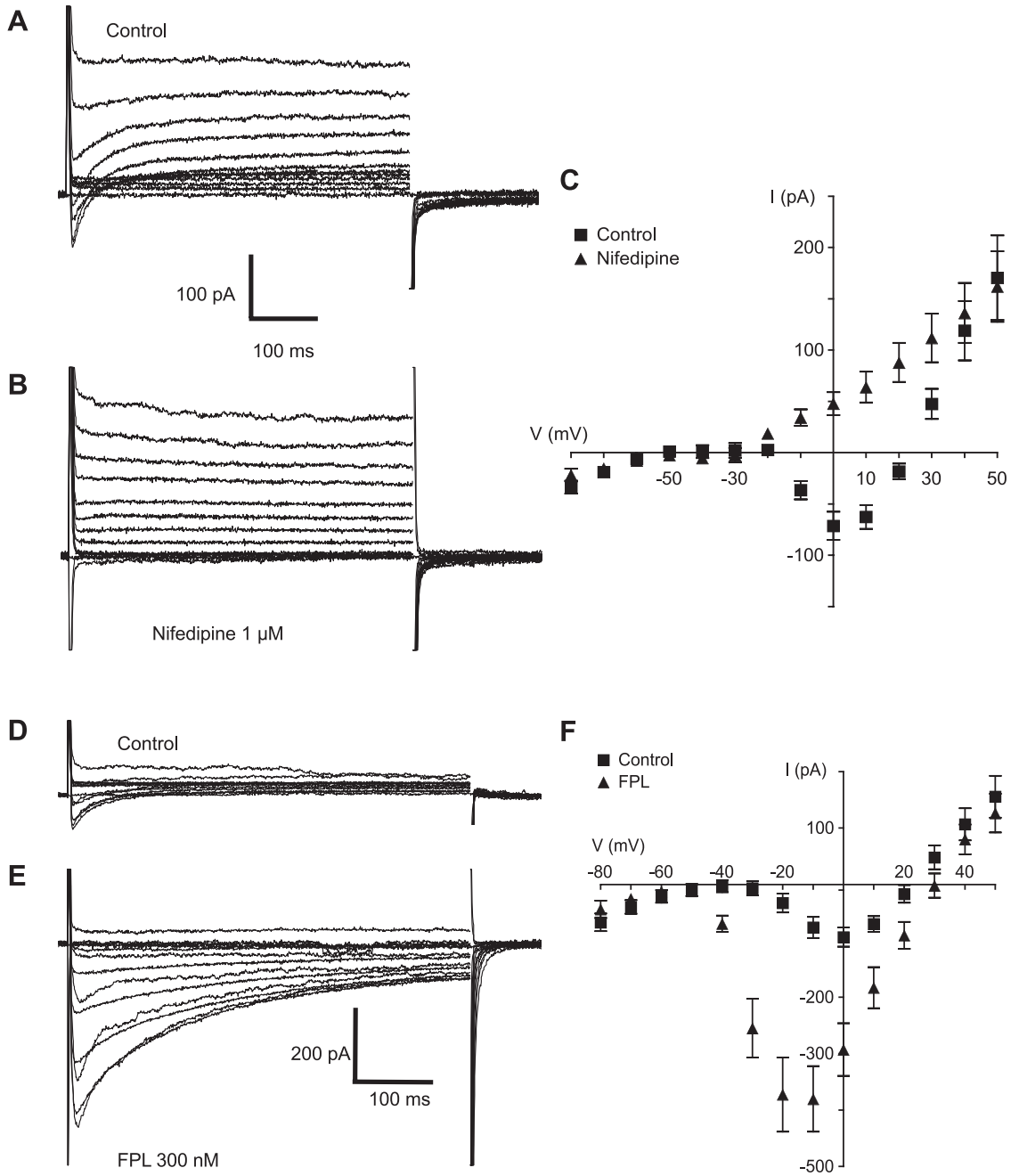

Fig. 5. *A* and *B*: family of currents (evoked by the same protocol as that described in Fig. 4) before (*A*) and in the presence of nifedipine (*B*). The transient inward current was blocked, indicating that it was an L-type calcium current. *C*: summary of 6 such experiments. Mean inward current (■) peaked at 0 mV and reversed at +23 mV. In the presence of nifedipine, inward current was abolished, leaving only the outward current carried by Cs^+. *D* and *E*: effects of the calcium channel agonist FPL-64176. The control inward currents (*D*) were greatly enhanced by 300 nM FPL 64176 (FPL; *E*). This was accompanied by somewhat slower activation kinetics and by very much slower inactivation, such that the currents were not fully inactivated at the end of the 500-ms sweep. *F*: a summary of 12 such experiments showing that the mean peak inward current increased in amplitude and that the voltage at which current peaked shifted negatively by 10 mV. Peak inward current increased by 308% from a control value (■) of 93 ± 17 pA to 380 ± 58 pA in the presence of FPL (▲; $n = 12$; $P < 0.001$).

attenuated in the presence of 1 mM 4-aminopyridine (4-AP) (Fig. 6*B*). Figure 6*C* summarizes the *I-V* plot for eight experiments in control conditions (closed squares) and in the presence of 4-AP (closed triangles). The current activated at −50 mV and showed outward rectification upon stepping to more positive potentials. 4-AP reduced the maximum current (at +50 mV) by 73% ($n = 8$, $P < 0.0001$). Similar results were also observed upon application of another potassium channel blocker, TEA. Mean peak current upon stepping to +50 mV was reduced from 1,625 ± 238 pA to 776 ± 127 pA in the presence of 1 mM TEA, a mean reduction of 52% ($n = 9$; $P < 0.001$).

Figure 6*D* shows the activation and inactivation properties of the delayed rectifier current. The current activated (closed squares) at potentials positive to −80 mV and was maximally active at +40 mV. $V_{1/2}$ of activation was −21 ± 0.7 mV ($n =$

Downloaded from ajpcell.physiology.org on March 8, 2012

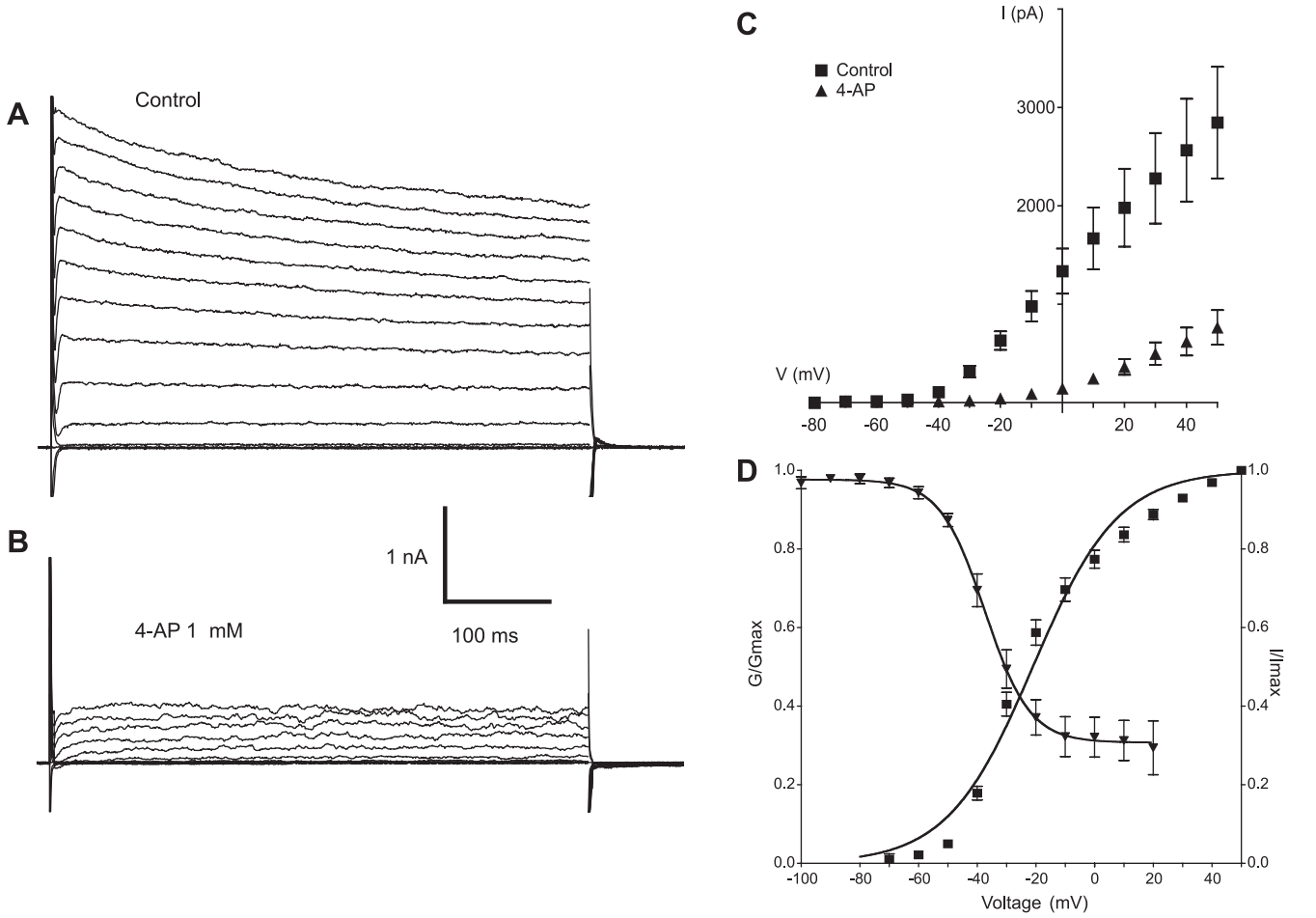

Fig. 6. *A*: family of outward currents evoked by the protocol described previously but using K^+ pipettes. The outward current activated rapidly and then relaxed slowly throughout the remainder of the 500-ms test pulse. *B*: the currents were greatly attenuated in the presence of 1 mM 4-aminopyridine (4-AP). *C*: summary of the current-voltage plot for eight experiments in control conditions (■) and in the presence of 4-AP (▲). The current activated at −50 mV and showed outward rectification upon stepping to more positive potentials. 4-AP reduced the maximum current by 73% ($n = 8$, $P < 0.0001$). *D*: current activation and inactivation properties. The current activated (■) at potentials positive to −80 mV and was maximally active at +40 mV. $V_{1/2}$ of activation was −21 ± 0.7 mV ($n = 38$). An inactivation protocol (conditioning pulses of 2-s duration in the range −100 to +20 mV stepping to a test potential of +40 mV) yielded the inactivation curve (▲). Inactivation began at potentials positive to −70 mV and reached a plateau at about 0 mV although 30% of the current was still available.

38). Inactivation (closed triangles) began at potentials positive to −70 mV and reached a plateau at about 0 mV, although 30% of the current was still available. This failure to inactivate completely is common to delayed rectifiers in many other cell types. $V_{1/2}$ of inactivation (conditioning pulses of 2-s duration in the range −100 to +20 mV stepping to a test potential of +40 mV for 500 ms) was −37 ± 1.4 mV ($n = 7$).

The reversal potential of the tail currents was measured to determine whether the voltage-dependent current was carried by potassium ions. Cells were stepped to +40 mV to activate the current, then returned to a number of test potentials from −100 mV in 10-mV increments to enable tail current recording. The reversal potential was taken as the point at which the *I-V* curve intersected the voltage axis. In normal extracellular solution (5.8 mM K^+) the tail current reversed at −65 ± 1 mV in eight cells. When the concentration of extracellular K^+ was raised to 60 mM, the reversal potential shifted to −18 ± 1 mV in five cells, not far from the calculated Nernst E_k of −21 mV. These results indicated that the outward current was carried mainly by K^+ ions.

The above results indicated that the outward current was a voltage-activated delayed rectifier potassium current so it was of interest to determine which channel types might be responsible for this conductance. Kv1 subunit expression was examined in cDNA from *passage 6* synoviocytes. Products of appropriate size were obtained for Kv1.1, Kv1.4, Kv1.5, and Kv1.6 following 35 cycles of PCR amplification ($n = 3$) (Fig. 7*A*). No expression for Kv1.2, Kv1.3, Kv1.7, or Kv1.8 was ever detected. As a positive control, we repeated the above PCR examination on rabbit brain cDNA. All eight Kv1 family subtypes were detected (Fig. 7*B*).

In view of the above findings it seemed likely that the expression of certain Kv1 subtypes was responsible for the synoviocyte outward current. Correolide, originally believed to be a specific Kv1.3 blocker (18), also blocks other Kv1 channels, albeit with a lower potency (24). Correolide was used to assess the contribution of Kv1 channels in our outward current. The control family of outward currents is shown in Fig. 8*A*. Application of 1 μM correolide caused a marked reduction in the peak outward currents at each voltage at which

Downloaded from ajpcell.physiology.org on March 8, 2012

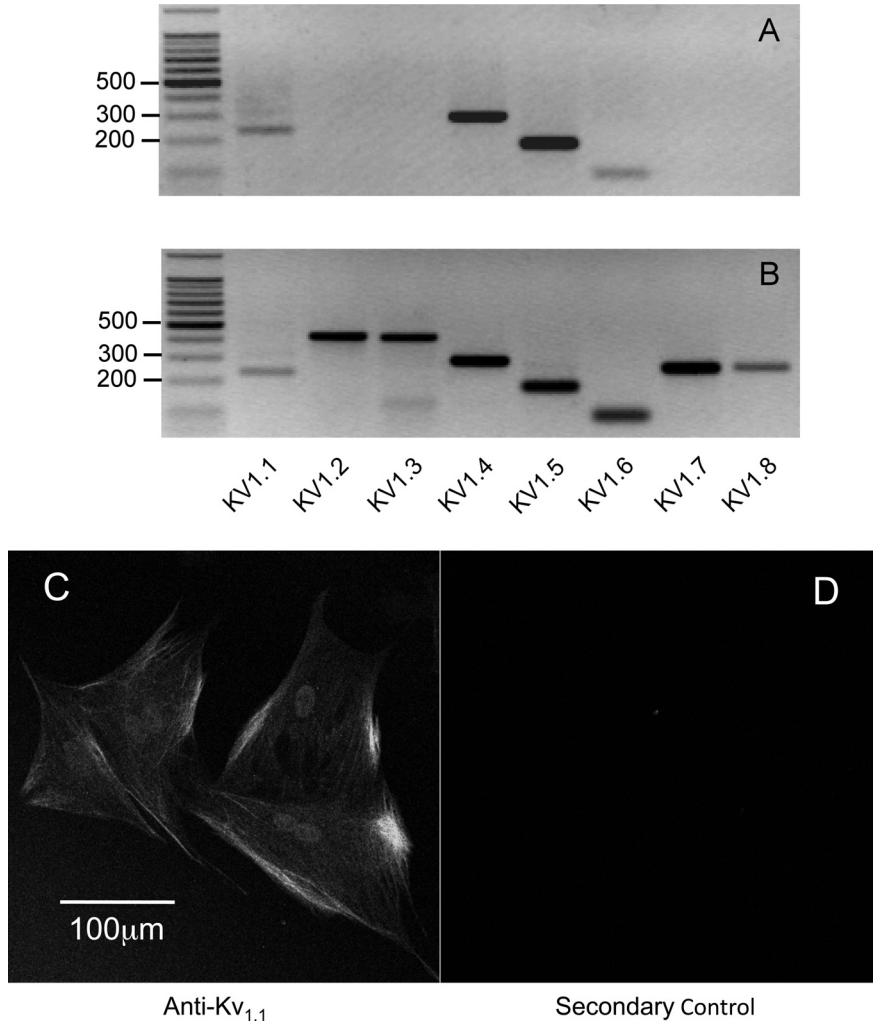

Fig. 7. Kv1 subunit expression in cDNA from *passage 6* synoviocytes. *A*: products of appropriate size were obtained for Kv1.1, Kv1.4, Kv1.5, and Kv1.6 following 35 cycles of PCR amplification ($n = 3$). *B*: as a positive control, cDNA from rabbit brain was examined using the same primers. All eight Kv1 subtypes were found in rabbit brain. *C* and *D*: immunostaining with a mouse monoclonal antibody against Kv1.1 (*C*) and the control experiment with only secondary antibody present (*D*).

the channel is active (Fig. 8*B*). The *I-V* plot summarizing five such experiments is shown in Fig. 8*C*. Mean peak control current at a step to +50 mV was reduced by 76% in the presence of 1 μm correolide, from 2,602 ± 643 pA to 601 ± 193 pA ($n = 5$; $P < 0.0002$).

Similar results were also obtained when we applied another generic Kv1 channel blocker, margatoxin. Treatment with 100 nM margatoxin again resulted in a 76% reduction in the mean peak outward current evoked by stepping from −60 mV to +50 mV ($n = 7$; $P < 0.0001$). The effects of both correolide and margatoxin further strengthened the hypothesis that the outward current was carried by K^+ efflux through Kv1 channels. To investigate this further, we used pharmacological antagonists of specific Kv1 subtypes. α-Dendrotoxin inhibits homo- and heteromultimeric channels composed of Kv1.1, Kv1.2, and Kv1.6, but not channels containing Kv1.5. (25). As shown in Fig. 8, *D*, *E*, and *F*, α-dendrotoxin (100 nM) reduced the control outward currents (at +50 mV) from 1,190 ± 183 pA to 312 ± 26 pA, a reduction of 74% ($n = 5$; $P < 0.0001$). The contribution of Kv1.1 to synoviocyte outward current was investigated by application of κ-dendrotoxin. As a specific inhibitor of both homo- and heteromultimeric Kv channels containing Kv1.1, κ-dendrotoxin was an ideal pharmacological tool for this purpose (26, 59). Figure 8, *G* and *H*, shows that the application of 50 nM κ-dendrotoxin almost completely abolished the family of outward potassium currents. The *I-V* plot summarizing four such experiments is shown in Fig. 8*I*. Under control conditions, with a holding potential of −60 mV, stepping to a test potential of +50 mV evoked a mean peak outward current of 2,451 ± 624 pA. This was dramatically reduced to 162 ± 28 pA upon application of 50 nM κ-dendrotoxin, a mean reduction of 93% ($n = 4$; $P < 0.0003$). Consistent with these pharmacological results was the observation that Kv1.1 expression could be demonstrated using a monoclonal antibody specific for Kv1.1 (Fig. 7*C*).

The results presented so far demonstrate the presence of both an inward L-type calcium current and an outward voltage-gated "delayed rectifier" potassium current of which Kv1.1 is a major constituent, in cultured rabbit intimal synoviocytes. One might hypothesize that the outward Kv current controls the synoviocyte membrane potential and that inhibition of this current would depolarize the cell, and thus activate the L-type calcium channels. No direct evidence has been presented thus far in support of this speculation, however, experiments such as those shown in Figs. 9 and 10 do provide such evidence. When the potassium concentration in Hanks' solution was increased to 60 mM (which is known to depolarize the cell by ~30 mV), there was a large rise in intracellular calcium. That this was

Downloaded from ajpcell.physiology.org on March 8, 2012

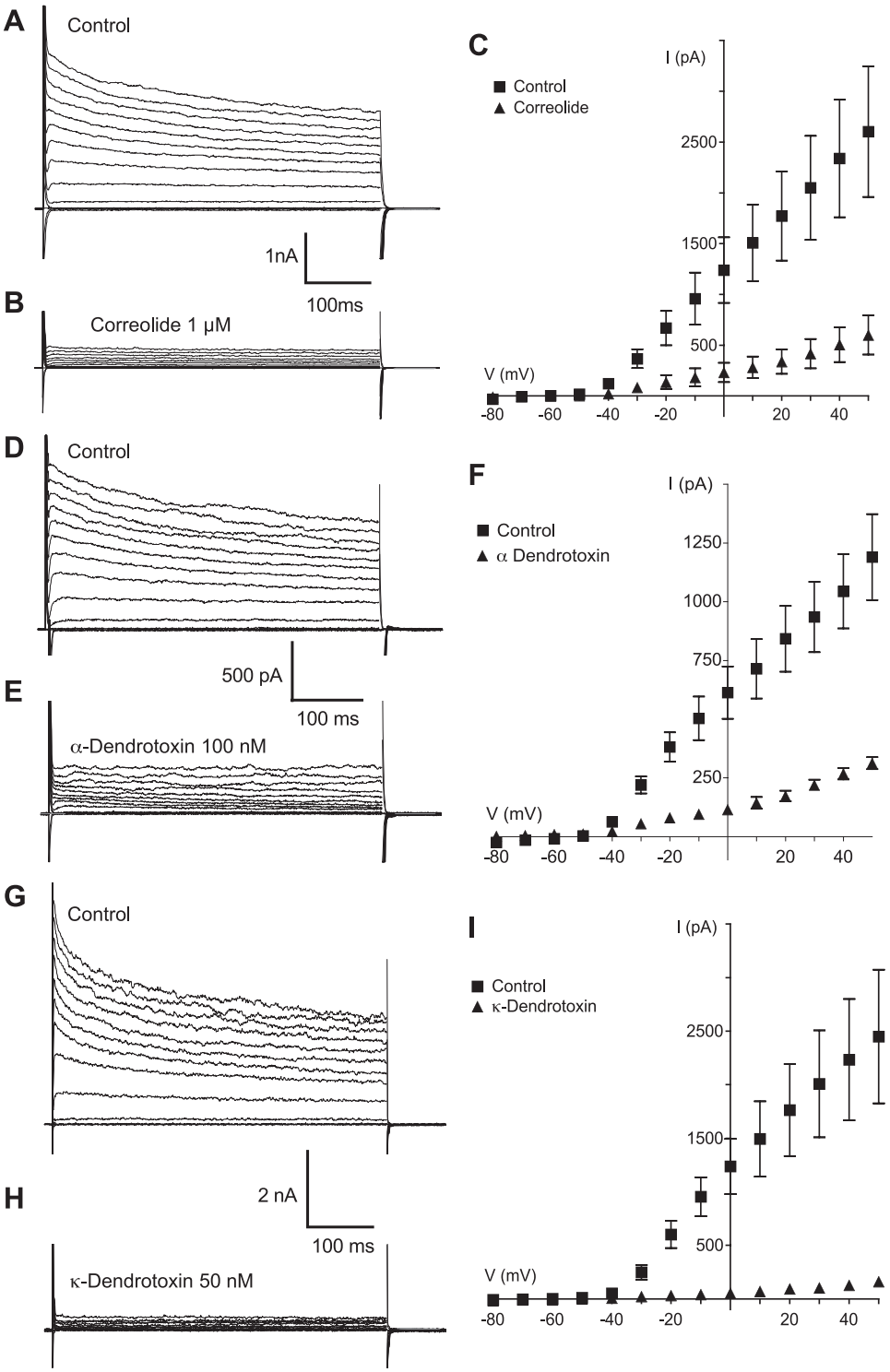

Fig. 8. Outward currents under control conditions are shown in *A*, *D*, and *G* while those in the presence of correolide (1 μM), α-dendrotoxin (100 nM), and κ-dendrotoxin (50 nM) are shown in *B*, *E*, and *H*. respectively. The most potent blocking effect by far was that of κ-dendrotoxin, which almost completely eliminated the current. The results for each set of experiments are summarized in the current-voltage plots of *C*, *F*, and *I*.

due, at least in part, to the opening of L-type calcium channels was confirmed by the observation that the response was greatly attenuated in the presence of 1 μM nifedipine. In three such experiments, the mean was 3.5 ± 2.2 in the presence of high potassium solution.

Similarly, the experiment shown in Fig. 10*A* suggests that Kv1.1 is important in the regulation of resting membrane potential. Addition of 50 nM κ-dendrotoxin to a current-clamped synoviocyte caused a >20-mV depolarization. In three such experiments, mean resting potential was −42.4 ± 4.6 mV, and this depolarized to a mean of −21.2 ± 3.7 mV in the presence of κ-dendrotoxin. That this depolarization was associated with an increase in calcium influx is shown in Fig. 10*B*. The *top* panel is a montage of a fluo-4-loaded synoviocyte imaged at the times shown. Addition of 50 nM κ-dendrotoxin caused a rapid rise in intracellular calcium which was largely

Downloaded from ajpcell.physiology.org on March 8, 2012

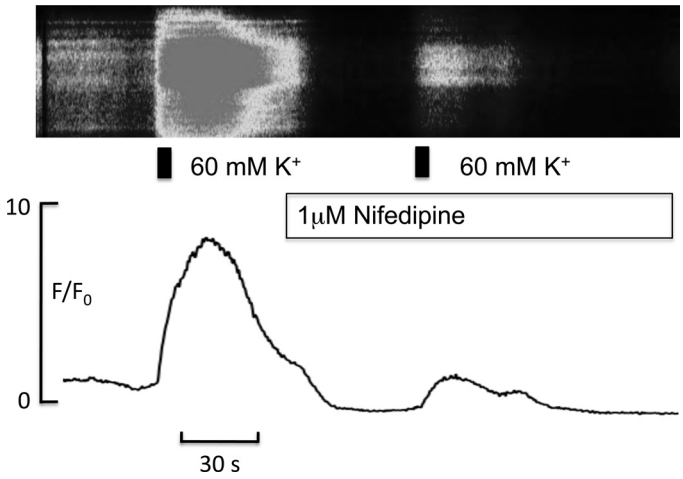

Fig. 9. *Top*: pseudo linescan of a synoviocyte loaded with the calcium indicator fluo-4 (see MATERIALS AND METHODS); shown are the effects of increasing external K^+ concentration for 5 s (indicated by the black bar) before and in the presence of 1 μM nifedipine. *Bottom*: F/F_0 plot of the same experiment. Depolarization of the membrane with high potassium caused a large increase in intracellular calcium, and this effect was greatly attenuated in the presence of nifedipine.

maintained during the period of drug administration. In six such experiments the mean change in F/F_0 in the presence of 50 nM κ-dendrotoxin was 3.76 ± 1.0.

DISCUSSION

Nature of Tissue Studied

This study is the first, to our knowledge, to investigate the electrophysiology of true, fibroblast-like synoviocytes, i.e., the synoviocytes that constitute the ~20 μm thick membrane lining the joint cavity. To harvest this very thin layer, microdissection is essential (56). Previous studies have used either a commercially available immortal cell line (37, 39) or cultured cells derived from gross dissection of the cavity-facing tissue (often in arthritic joints), which is likely to include a high proportion of tissue from the much thicker (>100 μm) subsynovial connective tissue layer and/or pathological tissue. In normal synovium the density of fibroblast-like synoviocytes declines sharply with distance from the joint cavity (57). Microdissection of the very thin synovial intima is thus essential, to harvest predominantly the intimal synoviocytes responsible for HA secretion. The test for NSE negativity, vimentin positivity and HAS2 expression indicated that the cells at *passage 6* had characteristics typical of FLS cells and not the other major synovial lining cell line, the macrophage.

Previous Work Implicating Intracellular Ca^{2+} in the Regulation of Synoviocyte HA Secretion

A major role of FLS cells is the production of HA, which is crucial for several functional properties of synovial fluid (lubrication, viscosity) and for the regulation of synovial lining permeability (48). Mechanical deformation, either by static or cyclical stretch, increases the rate of HA production in both intact joints (14, 29) and cultured rabbit intimal synoviocytes (52), demonstrating that synoviocytes exhibit a mechanosensitive response. Ca^{2+} appears to be an important component of the signal pathways regulating the HA secretion rate. For example, the Ca^{2+} ionophore A23187 stimulates HA production in 3T3 fibroblasts (36) and orbital fibroblasts in vitro (70). Moreover, the Ca^{2+} ionophore ionomycin, when injected into the cavity of rabbit knee joints, greatly increases the rate of intra-articular HA secretion in vivo (30). Cyclic movement of the joint stimulates HA production by a similar amount. Momberger et al. (53) showed that FLS cells cultured from microdissected rabbit synovium retain their mechanosensitivity in vitro (showing that they retain a specialized phenotype) and that the activation and translocation of a Ca^{2+}-dependent PKC isoform, PKCα, is an important element in the mechanosensitive signal pathway. Chelation of either extracellular or intracellular Ca^{2+} inhibited the secretory response, demonstrating a role for extracellular Ca^{2+} influx. When unstretched (control) or stretched cultured synoviocytes were exposed to medium containing BAPTA-AM, a membrane-permeant chelator of intracellular calcium, the HA secretion fell by 33%. Application of medium containing 10 μM EGTA, an extracellular chelator of calcium, likewise reduced net HA secretion in stretched cultured synoviocytes. A role for L-type calcium channels was supported by studies using Bay K, a dihydropyridine analog that prolongs L-type Ca channel open time, leading to an influx of extracellular Ca^{2+}. Bay K increased HA secretion in stretched cultured synoviocytes by 61% (53). Bay K also enhanced PKC activation and triggered the phosphorylation of its downstream effector ERK1/2. Inhibition of MEK-activated ERK1/2 blocked hyaluronan secretion. This led Momberger et al. (53) to suggest that L-type, nifedipine-sensitive Ca^{2+} channels might exist in functionally important

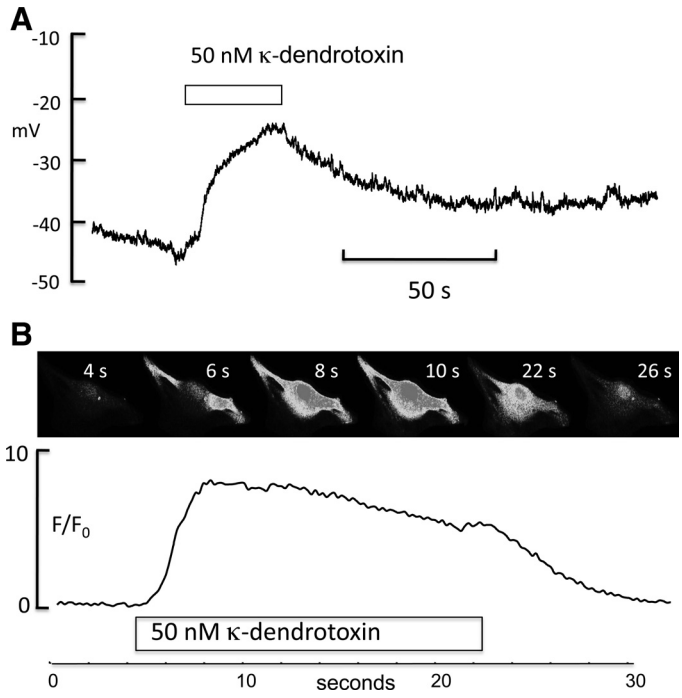

Fig. 10. *A*: synoviocyte in current clamp with a resting membrane potential between −50 and −40 mV. When 50 nM κ-dendrotoxin was added, the cell depolarized by >20 mV, suggesting a role for Kv1.1 channels in the maintenance of resting membrane potential. *B*: montage of a fluo-4-loaded synoviocyte to which 50 nM κ-dendrotoxin was added after 4 s. Intracellular calcium levels rose to a peak between 8 and 10 s, and this was well maintained until the toxin was removed, whereupon it fell to control levels as shown by the F/F_0 plot below.

Downloaded from ajpcell.physiology.org on March 8, 2012

numbers in the plasmalemma of cultured intimal synoviocytes and trigger the Ca^{2+}-PKCα-MEK-ERK1/2 cascade. They also pointed out that no direct, electrophysiological evidence existed to support this inference. This dearth of direct evidence provided the main stimulus for the present study. In subsequent studies of the regulatory pathways in intact synovium of rabbit knees in vivo, it was found that the inhibition of both the PKC-MEK-ERK1/2 cascade and the parallel p38 MAP kinase pathway was necessary to block the mechanosensitive stimulation of HA secretion (30).

Present Evidence for L-Type Ca^{2+} Channels in Cultured Synoviocytes

Our present findings provide the first direct evidence for the existence of L-type Ca^{2+} channels in cultured intimal synoviocytes. We have shown the presence of a voltage-sensitive inward current with activation/inactivation kinetics typical of the L-type calcium channel. The current is nifedipine sensitive and is completely abolished by the removal of extracellular calcium. In addition, application of FPL, a specific L-type voltage-gated calcium channel modulator, caused a large increase in the peak inward current. Together, these findings indicate the presence of L-type calcium channels in cultured synoviocytes.

Possible Functional Significance of L-Type Ca^{2} Channels in Nonexcitable Cells

The demonstration of L-type Ca^{2+} channels in FLS cells and in some other nonexcitable cells (see below) raises the question of their functional role. For example, do these voltage-activated channels contribute substantially as a calcium influx pathway? The observations of Momberger et al. (53), namely, that the L-type Ca^{2+} channel activator Bay K stimulates HA secretion in vitro, indicate a potential functional role in cultured synoviocytes. In conjunction with the new results presented here it could be hypothesized that stretch leads to the activation of L-type calcium channels, and that the resulting extracellular calcium influx activates the Ca^{2+}-sensitive PKC dependent pathway that regulates HA production. An alternative or complementary source of intracellular calcium could be the intracellular store, since an inhibitor of phospholipase C (PLC) almost completely eliminated movement-stimulated HA secretion in vivo (30). PLC acts upstream of the classic PKCα isoform, activating it through the formation of diacyl glycerol and inositol 1,4,5-trisphosphate-driven release of stored intracellular Ca^{2+}. A regulatory role for increases in intracellular Ca^{2+} is supported by a large increase in HA secretion into intact joints following treatment with intra-articular calcium ionophore (ionomycin)—an increase similar in magnitude to that evoked by cyclic movement. However, not all the available evidence supports a direct role for L-type Ca^{2+} channels in regulating HA secretion in vivo. In the rabbit knee joint model of Ingram et al. (30), intra-articular treatment with L-type calcium channel agonists, either Bay K or FPL, did not significantly stimulate HA secretion in static joints. Moreover, verapamil, an inhibitor of L-type calcium channels, did not inhibit the movement-stimulated HA secretion. A possible explanation for the latter finding, based on the PLC inhibition results, is that store release alone can provide a sufficient rise in intracellular Ca^{2+} to stimulate HA production. The lack of effect of L-type channel activators in vivo may be related to the difficulty in controlling drug concentration accurately in a living joint, or to a lower expression of the channels in vivo than in vitro.

The L-type Ca^{2+} channel is best known for its association with regenerative electrical activity in excitable tissues such as myocardium and smooth muscle. Nevertheless, L-type Ca^{2+} channels have been reported in many other nonexcitable cells besides synoviocytes, namely, endocrine cells, osteoblasts, retinal pigment epithelial cells, plasma cells, mast cells, and lymphocytes (21, 32, 33, 41, 50, 51), though their role in these cells is controversial (3, 42). The latter authors monitored membrane potential in T-lymphocytes using voltage-sensitive dye and detected a small nifedipine-sensitive depolarization in antigen-stimulated cells. This was consistent with a voltage-sensing role for L-type channels. In later experiments, however, depolarization of CD4 T-cells with KCl did not lead to calcium influx (as it would in excitable cells), apparently contradicting their earlier conclusion. It is possible that the L-type channel plays a role in cell differentiation and signaling that is unrelated to its voltage dependence. Thus Gomez-Ospina et al. (22) showed that a COOH-terminal fragment of the L-type channel ($Ca_v1.2$) translocates to the nucleus and regulates the transcription of a variety of genes that are important for differentiation.

Both fibroblasts and tissue macrophages possess calcium channels that resemble L-type calcium channels (5, 8, 55). This led Aune (2) to file a US patent that proposed L-type calcium antagonists as a treatment for arthritis. He presented evidence that dihydropyridines, phenylalkylamines, and benzothiazepines were effective in treating adjuvant-induced arthritis in rats. Aune argued that blockade of L-type channels might prevent the release of inflammatory mediators by synoviocytes or inhibit the massive proliferation of synoviocytes that leads to pannus formation. Proliferating synoviocytes play a key role in the joint destruction associated with rheumatoid arthritis (28). An important contribution of the present work is that it provides direct electrophysiological evidence that intimal synoviocytes do indeed express L-type Ca^{2+} channels.

Outward Currents Through Voltage-Gated K^+ Channels in Synoviocytes; Channel Identification

This study is the first, to our knowledge, to demonstrate the presence of a voltage-dependent, delayed rectifier outward current in cultured rabbit synoviocytes. A shift in reversal potential from −65 mV to −18 mV upon increasing extracellular K^+ from 5.8 mM to 60 mM indicated that this outward current is carried mainly by K^+ ions. Further evidence includes the sensitivity of the outward current to millimolar concentrations of the classical K^+ channel blockers TEA and 4-AP.

Regarding the molecular identity of the channels, members of the Kv1 family [apart from Kv1.4, which displays the properties of an A-type current (23)] are known to be delayed rectifiers. PCR analysis revealed the expression of four members of the Kv1 family, namely, Kv1.1, Kv1.4, Kv1.5, and Kv1.6. Correolide (micromolar range) and margatoxin (nanomolar range), which were originally thought to be specific Kv1 subunit antagonists but are now believed to block all Kv1 subtypes, caused a marked reduction in the family of outward currents. This led us to focus further attention on Kv1 channels,

Downloaded from ajpcell.physiology.org on March 8, 2012

which can be composed of one or more subtypes, namely, Kv1.1, Kv1.4, Kv1.5, and/or Kv1.6. The dendrotoxin proteins isolated from mamba snake venoms have become accepted pharmacological tools in investigating Kv1 channel function. α-Dendrotoxin in the nanomolar range specifically blocked subtypes Kv1.1, Kv1.2, and Kv1.6 (25), and reduced the peak outward current by 74%, indicating a key role for Kv1.1 or Kv1.6 containing channels in carrying the current. However, the most striking finding was the response to κ-dendrotoxin, a protein that obliterates the function of any homomultimeric Kv1.1 channel or heteromultimeric K^+ channel containing a Kv1.1 subunit. At 50 nM, κ-dendrotoxin reduced the synoviocyte peak outward current by 93%. This result strongly implicates Kv1.1 in carrying the delayed rectifier outward K^+ current in cultured rabbit knee synoviocytes. The present results do not indicate definitively whether the current is carried by homomultimeric Kv1.1 channels or heteromultimeric combinations of Kv1.1, Kv1.5, and Kv1.6 forming a functional channel.

Physiological Significance of Voltage-Gated K^+ Channels in Synoviocytes

Voltage-gated potassium channels contribute to a range of functions in a wide range of cell types. The functions include solute and water transport (43), cell adhesion (31), cell volume regulation (44), apoptosis (11), and control of resting membrane potential and hence muscle tone in airway (19) and vascular smooth muscle (4, 13). Control of membrane potential appears also to be important in the regulation of differentiation in nonexcitable cells, as demonstrated in the adipogenic and osteogenic differentiation of mesenchymal stem cells (65). In the present study the delayed rectifier current was demonstrated in cultured synoviocytes. In many cell types, a major role of voltage-gated potassium channels is the control of resting membrane potential (27), which in turn is generally an important factor controlling calcium influx via voltage-dependent calcium channels. The voltage-dependent inactivation of our current indicates that, at a resting membrane potential of ~ -45 mV, a fraction of our current is available. On the basis of this, it is reasonable to propose that a possible role for the current in cultured rabbit synoviocytes is to regulate membrane potential. However, this would need to be investigated in more detail in further studies. The wide range of synoviocyte membrane potentials (Fig. 2) means that the available potassium current will vary from almost 100% at the maximum recorded potential, -66 mV, to $<50\%$ at the most depolarized potential, -30 mV. It is not clear why there is such a relatively large range of resting membrane potentials in the cultured synoviocytes, but one explanation might be that they are at different stages in the cell cycle. There is a strong relationship between membrane potential and mitotic activity in many cell types. For example, the resting membrane potentials of Chinese hamster V79, Neuro-2A neuroblastoma, and MCF-7 cells synchronized in early to middle G_1 phase were very depolarized (-5 to -25 mV), but the membrane potential hyperpolarized by as much as 30 mV during progression through G_1 and entry into S phase (69). Consistent with this is the observation that TEA, 4-AP, and quinine inhibit the mitogen-stimulated proliferation of T-lymphocytes (10, 15).

In summary, the results demonstrate the presence of both an inward L-type calcium current and an outward voltage-gated "delayed rectifier" potassium current of which Kv1.1 is a major constituent, in cultured rabbit intimal synoviocytes. In discussing a physiological role for these current, we hypothesized that the outward Kv current controls the synoviocyte membrane potential. Inhibition of this current would depolarize the cell and thus activate the L-type calcium channels. The depolarizing effect of κ-dendrotoxin and the effects of high potassium solutions are consistent with this hypothesis. Ca^{2+} influx through this channel, along with the PLC-mediated release of intracellular Ca^{2+} stores, could contribute to the activation a calcium-dependent pathway, most likely the PKCα-MEK-ERK1/2 cascade known to stimulate HA production. Clearly, much further work is required fully to test this hypothesis, both in our cultured synoviocyte cell model and in freshly isolated synoviocytes.

GRANTS

This research was supported by Welcome Trust Grant 076752/B/05/Z.

DISCLOSURES

No conflicts of interest, financial or otherwise, are declared by the authors.

REFERENCES

1. **Anggiansah CL, Scott D, Poli A, Coleman PJ, Badrick E, Mason RM, Levick JR.** Regulation of hyaluronan secretion into rabbit synovial joints in vivo by protein kinase C. *J Physiol* 550: 631–640, 2003.
2. **Aune TM.** Inhibition of arthritis by L-type calcium channel antagonists nimodipine, nisoldipine and nifedipine. *US patent 5478848*, 1995.
3. **Badou A, Jha MK, Matza D, Mehal WZ, Freichel M, Flockerzi V, Flavell RA.** Critical role for the beta regulatory subunits of Cav channels in T lymphocyte function. *Proc Natl Acad Sci USA* 103: 15529–15534, 2006.
4. **Bae YM, Kim A, Kim J, Park SW, Kim TK, Lee YR, Kim B, Cho SI.** Serotonin depolarizes the membrane potential in rat mesenteric artery myocytes by decreasing voltage-gated K^+ currents. *Biochem Biophys Res Commun* 347: 468–476, 2006.
5. **Baumgarten L, Villereal M.** Bradykinin stimulates Ca^{2+} entry via nitrendipine-sensitive Ca^{2+} channels in cultured human fibroblasts. *Agents Actions Suppl* 38: 1–8, 1992.
6. **Baxter AJ, Dixon J, Ince F, Manners CN, Teague SJ.** Discovery and synthesis of methyl 2,5-dimethyl-4-[2-(phenylmethyl)benzoyl]-1H-pyrrole-3-carboxylate (FPL 64176) and analogues: the first examples of a new class of calcium channel activator. *J Med Chem* 36: 2739–2744, 1993.
7. **Berg KD, Tamas RM, Riemann A, Niels-Christiansen LL, Hansen GH, Michael Danielsen E.** Caveolae in fibroblast-like synoviocytes: static structures associated with vimentin-based intermediate filaments. *Histochem Cell Biol* 131: 103–114, 2009.
8. **Bernini F, Bellosta S, Didoni G, Fumagalli R.** Calcium antagonists and cholesteryl ester metabolism in macrophages. *J Cardiovasc Pharmacol* 18, *Suppl* 10: S42–S45, 1991.
9. **Camelliti P, Borg TK, Kohl P.** Structural and functional characterisation of cardiac fibroblasts. *Cardiovasc Res* 65: 40–51, 2005.
10. **Chandy KG, DeCoursey TE, Cahalan MD, McLaughlin C, Gupta S.** Voltage-gated potassium channels are required for human T lymphocyte activation. *J Exp Med* 160: 369–385, 1984.
11. **Chin LS, Park CC, Zitnay KM, Sinha M, DiPatri AJ Jr, Perillan P, Simard JM.** 4-Aminopyridine causes apoptosis and blocks an outward rectifier K^+ channel in malignant astrocytoma cell lines. *J Neurosci Res* 48: 122–127, 1997.
12. **Christensen BN, Kochukov M, McNearney TA, Taglialatela G, Westlund KN.** Proton-sensing G protein-coupled receptor mobilizes calcium in human synovial cells. *Am J Physiol Cell Physiol* 289: C601–C608, 2005.
13. **Cogolludo A, Moreno L, Lodi F, Frazziano G, Cobeno L, Tamargo J, Perez-Vizcaino F.** Serotonin inhibits voltage-gated K^+ currents in pulmonary artery smooth muscle cells: role of 5-HT2A receptors, caveolin-1, and KV1.5 channel internalization. *Circ Res* 98: 931–938, 2006.

Downloaded from ajpcell.physiology.org on March 8, 2012

14. **Coleman PJ, Scott D, Ray J, Mason RM, Levick JR.** Hyaluronan secretion into the synovial cavity of rabbit knees and comparison with albumin turnover. *J Physiol* 503: 645–656, 1997.
15. **DeCoursey TE, Chandy KG, Gupta S, Cahalan MD.** Dihydropyridine-sensitive L-type calcium channels: facts and controversies. *Nature* 307: 465–468, 1984.
16. **Edwards JCW.** The biology of synovial cells. In: *Biology of the Synovial Joint*, edited by Archer CW, Caterson B, Benjamin M, Ralphs JR. Amsterdam: Harwood Academic, 1999, p. 225–233.
17. **Estacion M.** Characterization of ion channels seen in subconfluent human dermal fibroblasts. *J Physiol* 436: 579–601, 1991.
18. **Felix JP, Bugianesi RM, Schmalhofer WA, Borris R, Goetz MA, Hensens OD, Bao JM, Kayser F, Parsons WH, Rupprecht K, Garcia ML, Kaczorowski GJ, Slaughter RS.** Identification and biochemical characterization of a novel nortriterpene inhibitor of the human lymphocyte voltage-gated potassium channel, Kv1.3. *Biochemistry* 38: 4922–4930, 1999.
19. **Fleischmann BK, Washabau RJ, Kotlikoff MI.** Control of resting membrane potential by delayed rectifier potassium currents in ferret airway smooth muscle cells. *J Physiol* 469: 625–638, 1993.
20. **Glogauer M, Ferrier J, McCulloch CA.** Magnetic fields applied to collagen-coated ferric oxide beads induce stretch-activated Ca^{2+} flux in fibroblasts. *Am J Physiol Cell Physiol* 269: C1093–C1104, 1995.
21. **Gomes B, Savignac M, Moreau M, Leclerc C, Lory P, Guery JC, Pelletier L.** Lymphocyte calcium signaling involves dihydropyridine-sensitive L-type calcium channels: facts and controversies. *Crit Rev Immunol* 24: 425–447, 2004.
22. **Gomez-Ospina N, Tsuruta F, Barreto-Chang O, Hu L, Dolmetsch R.** The C terminus of the L-type voltage-gated calcium channel Ca(V)1.2 encodes a transcription factor. *Cell* 127: 591–606, 2006.
23. **Gutman GA, Chandy KG, Grissmer S, Lazdunski M, McKinnon D, Pardo LA, Robertson GA, Rudy B, Sanguinetti MC, Stuhmer W, Wang X.** International Union of Pharmacology. LIII. Nomenclature and molecular relationships of voltage-gated potassium channels. *Pharmacol Rev* 57: 473–508, 2005.
24. **Hanner M, Schmalhofer WA, Green B, Bordallo C, Liu J, Slaughter RS, Kaczorowski GJ, Garcia ML.** Binding of correolide to K(v)1 family potassium channels. Mapping the domains of high affinity interaction. *J Biol Chem* 274: 25237–25244, 1999.
25. **Harvey AL.** Twenty years of dendrotoxins. *Toxicon* 39: 15–26, 2001.
26. **Hatton WJ, Mason HS, Carl A, Doherty P, Latten MJ, Kenyon JL, Sanders KM, Horowitz B.** Functional and molecular expression of a voltage-dependent K(+) channel (Kv1.1) in interstitial cells of Cajal. *J Physiol* 533: 315–327, 2001.
27. **Hille B.** *Ion Channels of Excitable Membranes*. Sunderland, MA: Sinauer, 2001.
28. **Huber LC, Distler O, Tarner I, Gay RE, Gay S, Pap T.** Synovial fibroblasts: key players in rheumatoid arthritis. *Rheumatology (Oxford)* 45: 669–675, 2006.
29. **Ingram KR, Wann AK, Angel CK, Coleman PJ, Levick JR.** Cyclic movement stimulates hyaluronan secretion into the synovial cavity of rabbit joints. *J Physiol* 586: 1715–1729, 2008.
30. **Ingram KR, Wann AK, Wingate RM, Coleman PJ, McHale N, Levick JR.** Signal pathways regulating hyaluronan secretion into static and cycled synovial joints of rabbits. *J Physiol* 587: 4361–4376, 2009.
31. **Itoh K, Stevens B, Schachner M, Fields RD.** Regulated expression of the neural cell adhesion molecule L1 by specific patterns of neural impulses. *Science* 270: 1369–1372, 1995.
32. **Jha MK, Badou A, Meissner M, McRory JE, Freichel M, Flockerzi V, Flavell RA.** Defective survival of naive CD8+ T lymphocytes in the absence of the beta3 regulatory subunit of voltage-gated calcium channels. *Nat Immunol* 10: 1275–1282, 2009.
33. **Jorgensen NR, Teilmann SC, Henriksen Z, Civitelli R, Sorensen OH, Steinberg TH.** Activation of L-type calcium channels is required for gap junction-mediated intercellular calcium signaling in osteoblastic cells. *J Biol Chem* 278: 4082–4086, 2003.
34. **Kamkin A, Kiseleva I, Wagner KD, Lammerich A, Bohm J, Persson PB, Gunther J.** Mechanically induced potentials in fibroblasts from human right atrium. *Exp Physiol* 84: 347–356, 1999.
35. **Kamkin A, Kiseleva I, Wagner KD, Lozinsky I, Gunther J, Scholz H.** Mechanically induced potentials in atrial fibroblasts from rat hearts are sensitive to hypoxia/reoxygenation. *Pflügers Arch* 446: 169–174, 2003.
36. **Klewes L, Prehm P.** Intracellular signal transduction for serum activation of the hyaluronan synthase in eukaryotic cell lines. *J Cell Physiol* 160: 539–544, 1994.
37. **Kochukov MY, McNearney TA, Fu Y, Westlund KN.** Thermosensitive TRP ion channels mediate cytosolic calcium response in human synoviocytes. *Am J Physiol Cell Physiol* 291: C424–C432, 2006.
38. **Kohl P, Kamkin AG, Kiseleva IS, Noble D.** Mechanosensitive fibroblasts in the sino-atrial node region of rat heart: interaction with cardiomyocytes and possible role. *Exp Physiol* 79: 943–956, 1994.
39. **Kolomytkin OV, Marino AA, Sadasivan KK, Wolf RE, Albright JA.** Interleukin-1 beta switches electrophysiological states of synovial fibroblasts. *Am J Physiol Regul Integr Comp Physiol* 273: R1822–R1828, 1997.
40. **Kolomytkin OV, Marino AA, Sadasivan KK, Wolf RE, Albright JA.** Intracellular signaling mechanisms of interleukin-1β in synovial fibroblasts. *Am J Physiol Cell Physiol* 276: C9–C15, 1999.
41. **Koschak A, Reimer D, Huber I, Grabner M, Glossmann H, Engel J, Striessnig J.** alpha 1D (Cav1.3) subunits can form l-type Ca^{2+} channels activating at negative voltages. *J Biol Chem* 276: 22100–22106, 2001.
42. **Kotturi MF, Hunt SV, Jefferies WA.** Roles of CRAC and Cav-like channels in T cells: more than one gatekeeper? *Trends Pharmacol Sci* 27: 360–367, 2006.
43. **Lang F, Rehwald W.** Potassium channels in renal epithelial transport regulation. *Physiol Rev* 72: 1–32, 1992.
44. **Lee SC, Price M, Prystowsky MB, Deutsch C.** Volume response of quiescent and interleukin 2-stimulated T-lymphocytes to hypotonicity. *Am J Physiol Cell Physiol* 254: C286–C296, 1988.
45. **Levick JR, McDonald JN.** Ultrastructure of transport pathways in stressed synovium of the knee in anaesthetized rabbits. *J Physiol* 419: 493–508, 1989.
46. **Li GR, Sun HY, Chen JB, Zhou Y, Tse HF, Lau CP.** Characterization of multiple ion channels in cultured human cardiac fibroblasts. *PLoS One* 4: e7307, 2009.
47. **Lu Y, Levick JR, Wang W.** The mechanism of synovial fluid retention in pressurized joint cavities. *Microcirculation* 12: 581–595, 2005.
48. **Mason RM, Coleman PJ, Scott D, Levick JR.** Role of hyaluronan in regulating joint fluid flow. In: *The Many Faces of Osteoarthritis*, edited by Hascall VC and Kuettner KE. Basel: BirkHauser-Verlag, 2002, p. 179–187.
49. **McDonald JN, Levick JR.** Morphology of surface synoviocytes in situ at normal and raised joint pressure, studied by scanning electron microscopy. *Ann Rheum Dis* 47: 232–240, 1988.
50. **McRory JE, Hamid J, Doering CJ, Garcia E, Parker R, Hamming K, Chen L, Hildebrand M, Beedle AM, Feldcamp L, Zamponi GW, Snutch TP.** The CACNA1F gene encodes an L-type calcium channel with unique biophysical properties and tissue distribution. *J Neurosci* 24: 1707–1718, 2004.
51. **Mergler S, Strauss O.** Stimulation of L-type Ca(2+) channels by increase of intracellular InsP3 in rat retinal pigment epithelial cells. *Exp Eye Res* 74: 29–40, 2002.
52. **Momberger TS, Levick JR, Mason RM.** Hyaluronan secretion by synoviocytes is mechanosensitive. *Matrix Biol* 24: 510–519, 2005.
53. **Momberger TS, Levick JR, Mason RM.** Mechanosensitive synoviocytes: a Ca^{2+} -PKCalpha-MAP kinase pathway contributes to stretch-induced hyaluronan synthesis in vitro. *Matrix Biol* 25: 306–316, 2006.
54. **Ohno S, Tanimoto K, Fujimoto K, Ijuin C, Honda K, Tanaka N, Doi T, Nakahara M, Tanne K.** Molecular cloning of rabbit hyaluronic acid synthases and their expression patterns in synovial membrane and articular cartilage. *Biochim Biophys Acta* 1520: 71–78, 2001.
55. **Olsen DR, Peltonen J, Jaakkola S, Chu ML, Uitto J.** Collagen gene expression by cultured human skin fibroblasts. Abundant steady-state levels of type VI procollagen messenger RNAs. *J Clin Invest* 83: 791–795, 1989.

55a. **Plane F, Johnson R, Kerr P, Wiehler W, Thorneloe K, Ishii K, Chen T, Cole W.** Heteromultimeric Kv1 channels contribute to myogenic control of arterial diameter. *Circ Res* 96: 216–224, 2005.

56. **Price FM, Levick JR, Mason RM.** Glycosaminoglycan concentration in synovium and other tissues of rabbit knee in relation to synovial hydraulic resistance. *J Physiol* 495: 803–820, 1996.
57. **Price FM, Mason RM, Levick JR.** Radial organization of interstitial exchange pathway and influence of collagen in synovium. *Biophys J* 69: 1429–1439, 1995.

Downloaded from ajpcell.physiology.org on March 8, 2012

58. **Rae J, Cooper K, Gates P, Watsky M.** Low access resistance perforated patch recordings using amphotericin B. *J Neurosci Methods* 37: 15–26, 1991.
59. **Robertson B, Owen D, Stow J, Butler C, Newland C.** Novel effects of dendrotoxin homologues on subtypes of mammalian Kv1 potassium channels expressed in *Xenopus* oocytes. *FEBS Lett* 383: 26–30, 1996.
60. **Rose RA, Hatano N, Ohya S, Imaizumi Y, Giles WR.** C-type natriuretic peptide activates a non-selective cation current in acutely isolated rat cardiac fibroblasts via natriuretic peptide C receptor-mediated signalling. *J Physiol* 580: 255–274, 2007.
61. **Sabaratnam S, Mason RM, Levick JR.** Molecular sieving of hyaluronan by synovial interstitial matrix and lymphatic capillary endothelium evaluated by lymph analysis in rabbits. *Microvasc Res* 66: 227–236, 2003.
62. **Scott D, Coleman PJ, Abiona A, Ashhurst DE, Mason RM, Levick JR.** Effect of depletion of glycosaminoglycans and non-collagenous proteins on interstitial hydraulic permeability in rabbit synovium. *J Physiol* 511: 629–643, 1998.
63. **Scott D, Coleman PJ, Mason RM, Levick JR.** Concentration-dependence of interstitial flow buffering by hyaluronan in synovial joints. *Microvasc Res* 59: 345–353, 2000.
64. **Stevens CR, Mapp PI, Revell PA.** A monoclonal antibody (Mab 67) marks type B synoviocytes. *Rheumatol Int* 10: 103–106, 1990.
65. **Sundelacruz S, Levin M, Kaplan DL.** Membrane potential controls adipogenic and osteogenic differentiation of mesenchymal stem cells. *PLoS One* 3: e3737, 2008.
66. **Triggle D.** Pharmacology of CaV1 (L-type) calcium channels. In: *Calcium Channel Pharmacology*, edited by McDonough SI. New York: Kluwer Academic/Plenum, 2004, p. 21–72.
67. **Walsh KB, Zhang J.** Neonatal rat cardiac fibroblasts express three types of voltage-gated K^+ channels: regulation of a transient outward current by protein kinase C. *Am J Physiol Heart Circ Physiol* 294: H1010–H1017, 2008.
68. **Wann AK, Ingram KR, Coleman PJ, McHale N, Levick JR.** Mechanosensitive hyaluronan secretion: stimulus-response curves and role of transcription-translation-translocation in rabbit joints. *Exp Physiol* 94: 350–361, 2009.
69. **Wonderlin WF, Strobl JS.** Potassium channels, proliferation and G1 progression. *J Membr Biol* 154: 91–107, 1996.
70. **Wong YK, Tang KT, Wu JC, Hwang JJ, Wang HS.** Stimulation of hyaluronan synthesis by interleukin-1beta involves activation of protein kinase C betaII in fibroblasts from patients with Graves' ophthalmopathy. *J Cell Biochem* 82: 58–67, 2001.
71. **Wright MO, Stockwell RA, Nuki G.** Response of plasma membrane to applied hydrostatic pressure in chondrocytes and fibroblasts. *Connect Tissue Res* 28: 49–70, 1992.

Downloaded from ajpcell.physiology.org on March 8, 2012